Hindawi
Journal of Chemistry
Volume 2022, Article ID 3646375, 7 pages
https://doi.org/10.1155/2022/3646375

Research Article

IL-2 Flexible Loops Might Play a Role in IL-2 Interaction with the High-Affinity IL-2 Receptor: A Molecular Dynamics (MD) Study

Ahmed L. Alaofi

Department of Pharmaceutics, College of Pharmacy, King Saud University, Riyadh, Saudi Arabia

Correspondence should be addressed to Ahmed L. Alaofi; ahmedofi@ksu.edu.sa

Received 21 July 2022; Revised 4 October 2022; Accepted 14 October 2022; Published 1 November 2022

Academic Editor: Dharmendra Kumar Yadav

The clinical use of high-dose IL-2 in cancer immunotherapy faces several drawbacks such as toxicity and unfavorable pharmacokinetic profile. These drawbacks can be avoided by inhibiting IL-2 interaction with the CD25 subunit, which is a component of the high-affinity IL-2 receptor (IL-2R$\alpha\beta\gamma$). Several studies showed mutations of potential IL-2 residues such as R38, F42, Y45, and Y72 would produce IL-2 that is CD25-independent. In essence, structural comparison between wild-type (WT) IL-2 and CD25-independent IL-2 can be very insightful to assess the role of IL-2 flexibility and conformation in the IL-2 receptor interactions. Here, we investigated the flexibility loops and conformation of IL-2m (F24A, Y45A, and L72G), which is known to be CD25-independent, and IL-2m2 (F42Y and L72R) mutants along with WT IL-2 using MD simulations. Despite residue mutations, both IL-2m and IL-2m2 showed comparable conformational compactness and better stability than WT IL-2. Interestingly, IL-2m and IL-2m2 mutants showed rigid BC and CD loops in comparison to WT IL-2 . Also, the AB loop conformation of IL-2m was a bent structure compared to the WT IL-2 and IL-2m2. Principal component analysis (PCA) and free-energy landscape results suggested IL-2m and IL-2m2 have stable conformations compared to the WT IL-2. Therefore, these mutation sites of IL-2 produced stable and rigid loops that might prevent IL-2 from binding to the CD25 subunit. Our results can help to assess IL-2 flexibility loops to design new CD25-independent IL-2 mutants without compromising the IL-2 structure.

1. Introduction

Interleukin-2 (IL-2) is an immunoregulatory cytokine with a molecular weight of 15.5 kDa and four antiparallel α-helices structure that plays a crucial role in the immune response [1–3]. IL-2 exerts its stimulation function by binding to monomeric, dimeric, or trimeric IL-2 receptors (IL-2Rs). The high-affinity trimeric receptor (IL-2R$\alpha\beta\gamma$) of IL-2 consists of α (CD25), β (CD122), and γ (CD132) subunits, while the moderate-affinity dimeric receptor (IL-2R$\beta\gamma$) consists of β and γ subunits [4]. IL-2 acts as a lymphocyte growth and stimulating factor that promotes the expansion, differentiation, and survival of antigen-activated T cells and B cells as well as the cytolytic activity of natural killer (NK) cells and regulated T (Treg) cells [5, 6]. Therefore, the antitumor activity of IL-2 is attributed to its ability to expand and activate innate and adaptive effector cells. The high dose of IL-2 was used as an immunotherapy agent to eradicate cancer cells by expanding effector T cells and NK cells population in patients [7–9]. Recombinant IL-2 (aldesleukin) was the first immunotherapy agent to gain the FDA approval in 1992 to treat metastatic renal cancer and later for metastatic melanoma [10].

However, using IL-2 as a therapeutic agent is limited due to severe toxic effects such as capillary leak syndrome, hypotension, hypoxia, and neurological effects, as well as the induction of immunosuppressive responses and bearing a short half-life [2]. Also, IL-2 might induce pulmonary edema as a result of IL-2 binding to CD25 (IL-2Rα) on lung endothelial cells [11]. The CD25 subunit is highly expressed in Treg cells, thus binding of IL-2 to the high-affinity IL-2 receptor (i.e., IL-2R$\alpha\beta\gamma$) deviates the IL-2 activity toward expansion of Treg cells. This limits the bioavailability of IL-2 to stimulate antitumor effector T cells and NK cells [12]. Therefore, preventing IL-2 binding to CD25 (α subunit) can minimize its toxicity profile as a cancer immunotherapeutic

agent. On the other hand, expansion of Treg cells is required in the treatment of other diseases such as autoimmune diseases (AD); therefore, low dose of IL-2 treatment has been evaluated in clinical trials to treat AD [13–16].

In cancer immunotherapy, modified IL-2-based agents have been developed to avoid the abovementioned toxic effects and improve the pharmacokinetics (e.g., short half-life) and pharmacodynamic profiles. This can be achieved by maintaining or improving IL-2 binding to IL-2R$\beta\gamma$ receptor while abolishing or minimizing binding to IL-2R$\alpha\beta\gamma$ receptor. For instance, site-directed mutagenesis of IL-2 has been developed to lower its affinity to the high-affinity IL-2 receptor (CD25-independent IL-2). In previous work, F42K or R38A mutations in IL-2 decreased its affinity toward IL-2R$\alpha\beta\gamma$ receptor while maintaining the affinity toward IL-2R$\beta\gamma$ receptor [17, 18]. Another study showed that mutation of F24A, Y45A, and L72G residues abolished the IL-2 mutant (IL-2m) interaction with the CD25 subunit [19]. IL-2m (CD25-independent) was conjugated to a specific cergutuzumab amunaleukin (CEA) antibody to improve therapeutic and pharmacokinetic profiles of IL-2. Moreover, IL-2 mutation strategies can also strengthen small molecule inhibitors to block IL-2-CD25 interaction [20]. Other strategies such as adding polyethylene glycol (PEG), Fc domain of immunoglobulin (Ig) moieties, or specific antibodies to IL-2 would enhance the IL-2 half-life.

Protein conformations play a crucial role in their biological activities and binding interactions. The intrinsic flexibility of IL-2 plays a significant role in the IL-2 receptor interaction by modulating the strength of the binding interaction [21, 22]. Here, we assess IL-2 loop flexibility and conformations of IL-2m (i.e., CD25-independent IL-2) along with wild-type (WT) IL-2 using MD simulations. Also, we designed IL-2 mutant 2 (IL-2m2) by mutation of F42Y, and L72R residues to investigate the relationship between potential residues sites and IL-2 flexibility loops. The mutation of Y42 and R72 residues in IL-2m2 was based on their similarity to F42 and L72 residues in size and chemical structure as well as their position between AB loop and helix B. Comparative investigation of conformation and flexibility between WT and CD25-independent interleukins might be insightful to assess their loops roles in IL-2 structures. Thus, it allows researchers to design IL-2 mutants that do not bind to the CD25 subunit while maintaining the required conformation and stability along with the ability to interact with moderated-affinity IL-2 receptor.

2. Result and Discussion

2.1. IL-2 Flexibility. C-α root mean square deviation (RMSD) was used to assess the stability of MD simulations systems of WT IL-2, IL-2m, and IL-2m2 mutants. All systems reached convergence during the simulations and thereby stable systems were obtained (Figure 1(a)). The flexibility results of interleukin showed that IL-2m and IL-2m2 structures significantly have higher rigidity than the WT IL-2 in helix C, BC, and CD loops as well as slightly in the AB loop (Figure 1(b)). The dynamic of the AB loop is essential toward IL-2R$\alpha\beta\gamma$ binding; therefore, binding of antibodies or small molecule inhibitors to this loop prevents IL-2 interaction with IL-2R$\alpha\beta\gamma$ receptor [23]. Because of similar observed rigidity of IL-2m and IL-2m2 mutants, sites 42 and 72 might play an important role in the IL-2 flexibility despite residue types (Figure 2). Taking the intrinsic dynamics of IL-2 into account, our results suggest IL-2 might need the high flexibility loops to interact with IL-2R$\alpha\beta\gamma$. The flexibility of these loops might not be required to interact with IL-2R$\beta\gamma$ since IL-2m maintained its affinity toward IL-2R$\beta\gamma$. Although the absent interaction of IL-2m with IL-2R$\alpha\beta\gamma$ was attributed to the loss of potential residues in IL-2R interaction, our results suggest mutation of the sites 42 and 72 induced the loops rigidity of IL-2m.

2.2. IL-2 Conformation and Radius of Gyration (Rg). The intrinsic dynamic of IL-2 is well-known to play a role in their biological function; particularly during interaction with IL-2R [22, 24]. A single or multiple mutations in proteins can change proteins conformation and thereby their biological activity [25–27]. The BC and CD loops were rigid structures in the IL-2m mutant (CD25-indpendent) possibly because of removing F42 and L72 residues, which could act as hinders between the AB loop and helix B in the WT IL-2. Therefore, the AB loop showed bent structure in IL-2m compared to WT IL-2 and IL-2m2 (Figure 3). However, Y45 residue might play less role in the AB, BC, and CD loop structures since Y45 residue was not mutated in IL-2m2 mutant that showed similar loops rigidity compared to IL-2m mutant. Surprisingly, F42A, Y45A, L72G or F42Y, and L72R mutations did not change the Rg values in IL-2m or IL-2m2, respectively (Figure 4(a)). Rg values for WT IL-2, IL-2m, and IL-2m2 have similar values (around 1.52 nm). This indicated that the conformational compactness of the WT and its mutants were similar. Therefore, mutation sites (42, 45, and 72) might not influence the whole IL-2 conformation while influencing the IL-2 loops flexibility. This finding could help to design further CD25-independent IL-2 mutants without compromising IL-2 conformation or its stability.

2.3. Solvent Accessible Surface Area (SASA). The solvent accessible surface area (SASA) was assessed for IL-2m and IL-2m2 in comparison to WT IL-2 in this study [28, 29]. The SASA can estimate exposed or buried residues of IL-2 during the MD simulations. In consistent with Rg results, all-residue SASA values of WT IL-2, IL-2m, and IL-2m2 were similar, especially after 60 ns of simulations (Figure 4(b)). Therefore, similar conformation was maintained for WT IL-2, IL-2m, and IL-2m2 even though there were three or two mutated residues. We can suggest that the mutations at sites 42 and 72 might decrease the flexibility of IL-2 but not compromise their solvent exposure. Moreover, we elaborated further on SASA values in the AB loop residues in comparison to WT IL-2. Again, SASA of the AB loops were similar for both systems, especially after 90 ns of simulations (data not shown). Therefore, there were no conformational changes due the F42A, Y45A, and L72G mutation.

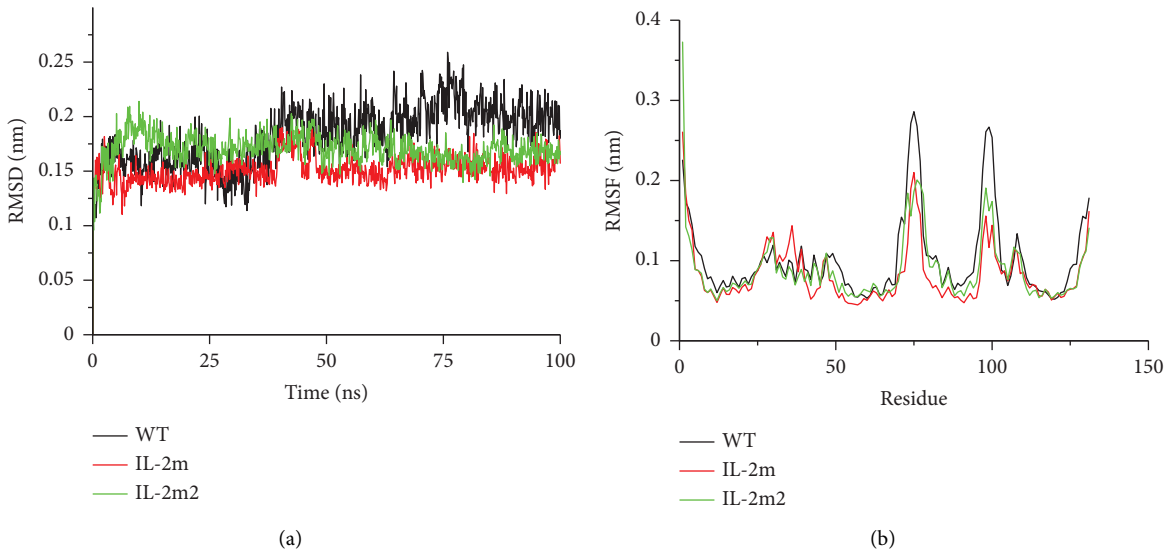

Figure 1: The C-α root mean square deviation (C-α RMSD) in nm as a function of simulations time in ps (a). C-α RMSD of WT IL-2 (black), IL-2m (red), and IL-2m2 (green) were depicted during the 100 ns MD simulations. Alignment of the C-α root mean square fluctuation (C-α RMSF) for WT IL-2 (black) with C-α RMSF of IL-2m (red) and IL-2m2 (green) (b). C-α RMSF values were depicted as a function of IL-2 residues. WT IL-2 showed higher flexibility in helix (c). AB, BC, and CD loops in comparison to other IL-2 mutants. The cartoon representation of IL-2 depicted with position of the AB, BC, and CD loops.

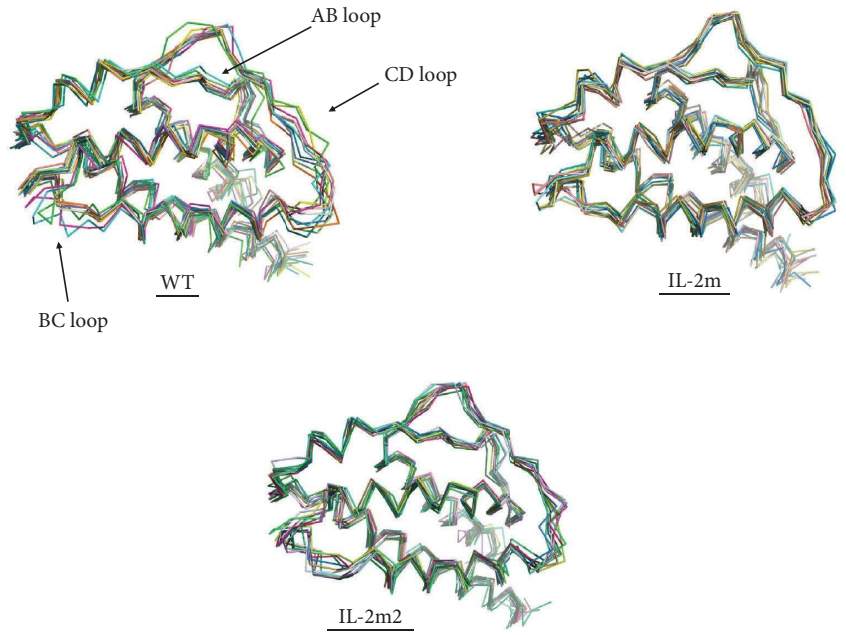

Figure 2: Ten frames each obtained every 10 ns for the 100 ns MD simulations were aligned together using ribbon representation for WT IL-2, IL-2m, or IL-2m2. The IL-2 loops were rigid in IL-2m and IL-2m2 compared to WT IL-2.

2.4. Principal Component Analysis (PCA). Due to the importance of IL-2 dynamics in its biological activities, we investigated the essential dynamics space on C-α of IL-2m (CD25-independent IL-2) and IL-2m2 along with WT IL-2 using the principal component analysis (PCA). Clearly, WT IL-2 covered a wider phase space than IL-2m by trajectories projection of the first principal components PC1 and PC2 (Figure 5). The PCA results suggest mutation of F42A, Y45A, and L72G in IL-2m might increase the stability by less flexibility observed in comparison to WT IL-2. Likewise, IL-2m2 showed similar PCA results of IL-2m; thus F42Y and L72R increased the structure stability. From a conformational dynamic perspective, IL-2m might not interact with IL-2R$\alpha\beta\gamma$ due to the observed dynamic and bent structure of the AB loop along with absence of potential binding-interacting residues (i.e., F42, Y45, and L72). Although IL-2m2 has not been tested experimentally yet, we assume IL-2m2 might be CD25-independent IL-2 based on our in silico

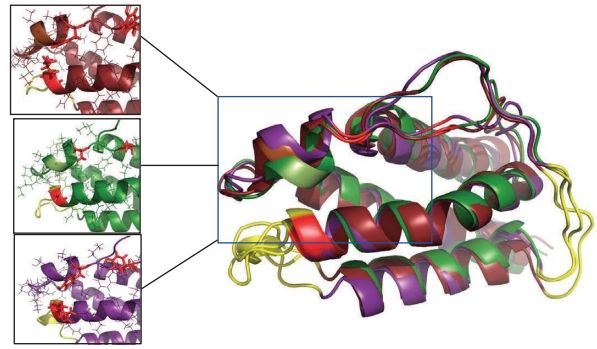

Figure 3: Alignment of 100 ns frames of WT IL-2 (ruby), IL-2m (forest), and IL-2m2 (deep purple). The small boxes showed the possible hinder of F42 and L72 in WT IL-2 (ruby) that was removed by F42A and L72G mutation in IL-2m (forest). For IL-2m2, Y42 and R72 might not cause the hinder since loops rigidity that was observed in IL-2m and IL-2m2.

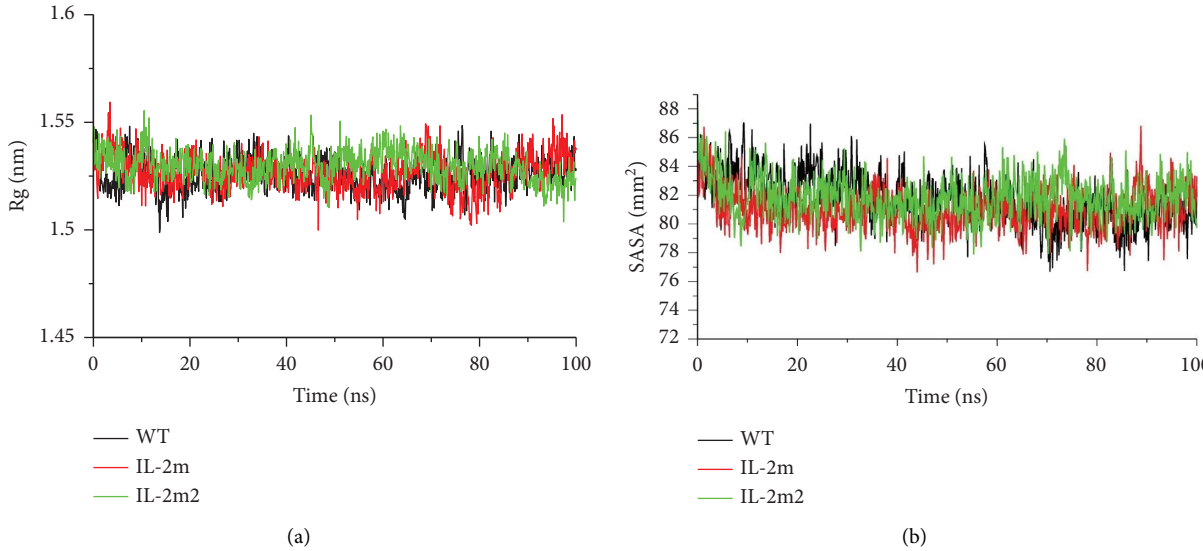

Figure 4: The radius of gyration (Rg) was plotted against simulation time (ps). Similar Rg values around 1.52 nm were obtained for WT IL-2 (black), IL-2m (red), and IL-2m2 (green) during the MD simulations (a). This indicates similar conformational compactness of WT IL-2 and IL-2m that reported as CD25-independent (i.e., not interacting with IL-2R$\alpha\beta\gamma$). Also, IL-2m2 showed similar conformational compactness. The surface area solvent accessibility (SASA) for WT IL-2 (black), IL-2m (red), and IL-2m2 (green) as a function of simulation time (b). There was no difference between WT IL-2 and its mutants.

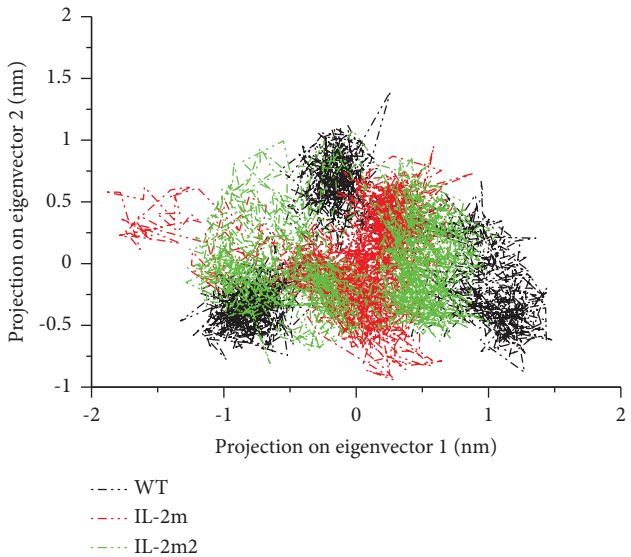

Figure 5: Projection of the motion of WT LI-2 (black) aligned with IL-2m (red) and IL-2m2 (green) mutant (red color) along with the first two principal eigenvectors (PC1 and PC2) in nm.

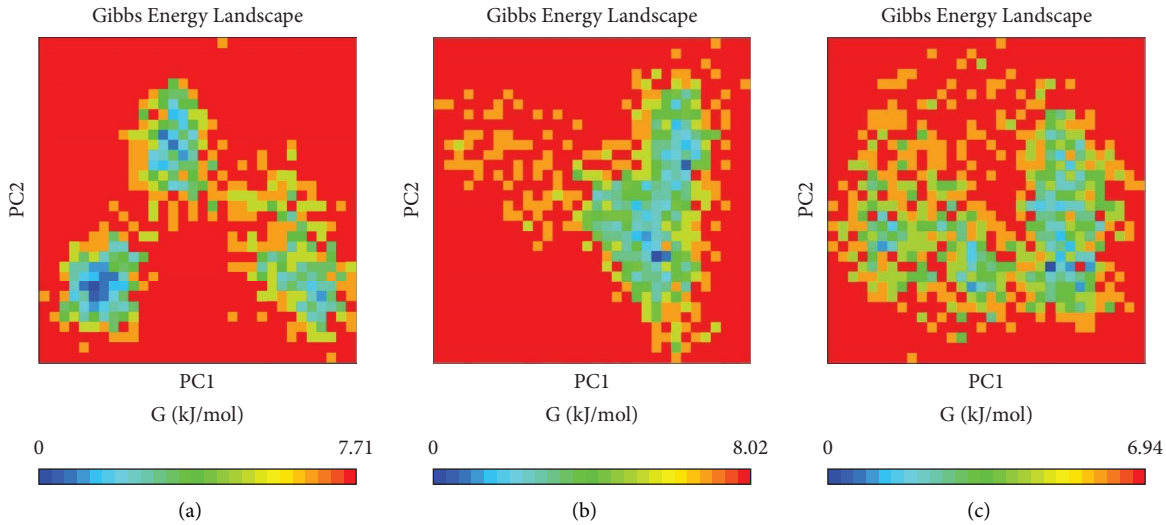

FIGURE 6: The free-energy landscape (FEL) was plotted using PC1 and PC2 for WT IL-2 (a), IL-2m (b), and IL-2m2 (c) during the 100 ns MD simulations. The FEL showed similar basins for IL-2m and IL-2m2 indicated for better stability.

results. This is due to similar effects of alanine compared to tyrosine and glycine compared to arginine in IL-2m and IL-2m2, respectively. Further, the free-energy changes were assessed using free-energy landscape (FEL) analysis for WT IL-2, IL-2m, and IL-2m2 through principal component plots. In consistent with previous results, IL-2m showed minima within a single basin while WT IL-2 showed wider basins (Figures 6(a)-6(b)). Therefore, these mutations in IL-2m might stabilize interleukin conformation. In previous work, IL-2m was prevented from interacting with IL-2R$\alpha\beta\gamma$ (high-affinity IL-2 receptor) while interacting with IL-2R$\beta\gamma$ [19]. For IL-2m2, we observed slightly similar basins in comparison to WT IL-2 (Figure 6(c)). This might be explained due to the chemical similarity of phenylalanine to tyrosine and lysine to arginine. Therefore, our finding suggests that mutation of IL-2m prevents IL-2R$\alpha\beta\gamma$ binding due to rigid and stable IL-2 structure especially in the potential loops.

3. Conclusion

The WT IL-2 binds to IL-2R$\alpha\beta\gamma$ and IL-2R$\beta\gamma$ receptors while IL-2m only binds to IL-2R$\beta\gamma$ receptor. Preventing IL-2 binding to IL-2R$\alpha\beta\gamma$ (α subunit known as CD25) receptor has clinical benefits due the known toxicity profile of IL-2. In our study, we performed a comparability study between conformation and flexibility of the WT IL-2 and its mutants IL-2m and IL-2m2 using MD simulations. Our results showed F42A and L72G mutation in IL-2m rigidified the BC, CD, and AB loops and maintained similar conformational compactness and solvent accessibility compared to WT IL-2. Moreover, IL-2m showed a better dynamic stability according to the PCA and FEL results. Therefore, we suggest rending IL-2 loops flexibility might play a role in the IL-2 interaction to IL-2R$\alpha\beta\gamma$. IL-2m2, F42Y, and L72R mutation produced similar flexibility and conformational results of IL-2m with less effect on the AB conformation. However, findings of our study can be confirmed using conformational and dynamic experimental studies such as fluorescence and H/D exchange instruments, respectively.

4. Material and Methods

4.1. Structure Preparation and MD Simulations. The structure of WT IL-2 was obtained from Protein Data Bank (PDB ID 1M47) [30]. Mutations of WT IL-2 to produce IL-2m (F42A, Y45A, and L72G) and IL-2m2 (F42Y and L72R) mutants were performed using PyMOL [31]. For molecular dynamic (MD) simulations, the X-ray structure and modeled structures were used as starting trajectories for WT IL and IL-2 mutants, respectively. Afterward, MD simulations was performed using GROMACS 5.1.4 program with CHARMM27 force field similar to our previous work with slight changes [26, 27, 32, 33]. Particle mesh Ewald (PME) [34] was used instead of the cutoff scheme, and a short-range nonbonded cutoff distance of 1.3 nm was used to compute the long-range electrostatic interactions. Then, solvation of all structures was done with TIP3P water [35] with the minimal distance of 0.407 nm between the solute and the wall of the cubic box the cubic box of length 7.47827 nm. Protonation states were assigned for titratable residues based on pH 7.0 condition using GROMACS pdb2gmx program. To mimic an ionic strength of 0.15 M, an equivalent amount of Na and Cl ions instead of water molecules was added. Then, a brief energy minimization (20 ps) followed by unconstrained equilibration MD simulation (100 ps) was done at a constant temperature (300 K) and pressure using Berendsen and Parrinello–Rahman coupling methods, respectively. Finally, for WT IL-2, IL-2m, and IL-2m2 solution structures production, a 100 ns-long production MD simulation at a constant temperature of 300 K was performed for each system; the temperature was controlled using a velocity-rescale thermostat and a time step of 2 fs.

4.2. Principal Component Analysis (PCA). PCA (known as essential dynamics analysis) has been utilized to filter large motions in macromolecules by reducing the number of dimensions that describe protein motions [36, 37]. To obtain PCA, first a covariance matrix was produced by using Cα atomic coordinates of WT, IL-2, and IL-2m2 trajectories. Then covariance matrix was diagonalized to produce eigenvalues and eigenvectors by gmx covar in GROMACS utilities as 85% of motion is cumulated in first 2 vectors. Finally, the first eigenvector, reflect WT, IL-2, and IL-2m2 motion behavior was visualized and used to plot the PCA.

4.3. Visualization and AnalysisF. MD simulation trajectories for each system were analyzed using GROMACS 5.6 tools. Root mean square of deviation (RMSD) and root mean square of fluctuation (RMSF) were calculated for WT IL-2, IL-2m, and IL-2m2 using *gmx rmsd* and *gmx rmsf*. For radius of gyration (Rg) and solvent accessible surface areaSFF (SASA), *gmx gyrate* and *gmx sasa* commands were used. All 2D plots were depicted using *xmgrace* in GROMACS utilities. PyMol was used to visualize and represent all IL-2 structures and to depict Porcupine plot (Sean M. Law et al.). Graphic visualization for WT IL-2 and its mutants were done using PyMOL 2.1.

Data Availability

All data generated or analyzed during this study are included in this published article.

Conflicts of Interest

The author declares that he has no conflicts of interest.

Acknowledgments

This work was supported by the Deanship of Scientific Research of King Saud University under Grant [R6-17-02-25].

References

[1] Z. Sun, Z. Ren, K. Yang et al., "A next-generation tumor-targeting IL-2 preferentially promotes tumor-infiltrating CD8+ T-cell response and effective tumor control," *Nature Communications*, vol. 10, no. 1, p. 3874, 2019.

[2] A. Tang and F. Harding, "The challenges and molecular approaches surrounding interleukin-2-based therapeutics in cancer," *Cytokine X*, vol. 1, Article ID 100001, 2019.

[3] S. Bird, J. Zou, T. Kono, M. Sakai, J. M. Dijkstra, and C. Secombes, "Characterisation and expression analysis of interleukin 2 (IL-2) and IL-21 homologues in the Japanese pufferfish, Fugu rubripes, following their discovery by synteny," *Immunogenetics*, vol. 56, no. 12, pp. 909–923, 2005.

[4] A. K. Abbas, E. Trotta, D. R Simeonov, A. Marson, and J. A. Bluestone, "Revisiting IL-2: biology and therapeutic prospects," *Science Immunology*, vol. 3, no. 25, Article ID eaat1482, 2018.

[5] R. Hernandez, J. Põder, K. M. LaPorte, and T. R. Malek, "Engineering IL-2 for immunotherapy of autoimmunity and cancer," *Nature Reviews Immunology*, vol. 22, no. 10, pp. 614–628, 2022.

[6] D. J. Stauber, E. W. Debler, P. A. Horton, K. A. Smith, and I. A. Wilson, "Crystal structure of the IL-2 signaling complex: paradigm for a heterotrimeric cytokine receptor," *Proceedings of the National Academy of Sciences*, vol. 103, no. 8, pp. 2788–2793, 2006.

[7] M. T. Lotze, L. W. Frana, S. O. Sharrow, R. J. Robb, and S. A. Rosenberg, "In vivo administration of purified human interleukin 2. I. Half-life and immunologic effects of the Jurkat cell line-derived interleukin 2," *Journal of Immunology*, vol. 134, no. 1, pp. 157–166, 1985.

[8] M. T. Lotze, Y. L. Matory, S. E. Ettinghausen et al., "In vivo administration of purified human interleukin 2. II. Half life, immunologic effects, and expansion of peripheral lymphoid cells in vivo with recombinant IL 2," *Journal of Immunology*, vol. 135, no. 4, pp. 2865–2875, 1985.

[9] S. A. Rosenberg, M. T. Lotze, L. M. Muul et al., "A progress report on the treatment of 157 patients with advanced cancer using lymphokine-activated killer cells and interleukin-2 or high-dose interleukin-2 alone," *New England Journal of Medicine*, vol. 316, no. 15, pp. 889–897, 1987.

[10] S. A. Rosenberg, J. C. Yang, D. E. White, and S. M. Steinberg, "Durability of complete responses in patients with metastatic cancer treated with high-dose interleukin-2: identification of the antigens mediating response," *Annals of Surgery*, vol. 228, no. 3, pp. 307–319, 1998.

[11] C. Krieg, S. Létourneau, G. Pantaleo, and O. Boyman, "Improved IL-2 immunotherapy by selective stimulation of IL-2 receptors on lymphocytes and endothelial cells," *Proceedings of the National Academy of Sciences*, vol. 107, no. 26, pp. 11906–11911, 2010.

[12] P. Berraondo, M. F. Sanmamed, M. C. Ochoa et al., "Cytokines in clinical cancer immunotherapy," *British Journal of Cancer*, vol. 120, no. 1, pp. 6–15, 2019.

[13] J. He, R. Zhang, M. Shao et al., "Efficacy and safety of low-dose IL-2 in the treatment of systemic lupus erythematosus: a randomised, double-blind, placebo-controlled trial," *Annals of the Rheumatic Diseases*, vol. 79, no. 1, pp. 141–149, 2020.

[14] M. Rosenzwajg, R. Lorenzon, P. Cacoub et al., "Immunological and clinical effects of low-dose interleukin-2 across 11 autoimmune diseases in a single, open clinical trial," *Annals of the Rheumatic Diseases*, vol. 78, no. 2, pp. 209–217, 2019.

[15] M. Mizui and G. C. Tsokos, "Low-dose IL-2 in the treatment of lupus," *Current Rheumatology Reports*, vol. 18, no. 11, p. 68, 2016.

[16] D. Saadoun, M. Rosenzwajg, F. Joly et al., "Regulatory T-cell responses to low-dose interleukin-2 in HCV-induced vasculitis," *New England Journal of Medicine*, vol. 365, no. 22, pp. 2067–2077, 2011.

[17] K. M. Heaton, G. Ju, and E. A. Grimm, "Human interleukin 2 analogues that preferentially bind the intermediate-affinity interleukin 2 receptor lead to reduced secondary cytokine secretion: implications for the use of these interleukin 2 analogues in cancer immunotherapy," *Cancer Research*, vol. 53, no. 11, pp. 2597–2602, 1993.

[18] K. M. Heaton, G. Ju, and E. A. Grimm, "Induction of lymphokine-activated killing with reduced secretion of interleukin-1 beta, tumor necrosis factor-alpha, and interferon-gamma by interleukin-2 analogs," *Annals of Surgical Oncology*, vol. 1, no. 3, pp. 198–203, 1994.

[19] C. Klein, I. Waldhauer, V. G. Nicolini et al., "Cergutuzumab amunaleukin (CEA-IL2v), a CEA-targeted IL-2 variant-based immunocytokine for combination cancer immunotherapy:

overcoming limitations of aldesleukin and conventional IL-2-based immunocytokines," *OncoImmunology*, vol. 6, no. 3, Article ID e1277306, 2017.

[20] C. D. Thanos, W. L. DeLano, and J. A. Wells, "Hot-spot mimicry of a cytokine receptor by a small molecule," *Proceedings of the National Academy of Sciences*, vol. 103, no. 42, pp. 15422–15427, 2006.

[21] A. M. Levin, D. L. Bates, A. M. Ring et al., "Exploiting a natural conformational switch to engineer an interleukin-2 "superkine"," *Nature*, vol. 484, no. 7395, pp. 529–533, 2012.

[22] V. S. De Paula, K. M. Jude, S. Nerli, C. R. Glassman, K. C. Garcia, and N. G. Sgourakis, "Interleukin-2 druggability is modulated by global conformational transitions controlled by a helical capping switch," *Proceedings of the National Academy of Sciences*, vol. 117, no. 13, pp. 7183–7192, 2020.

[23] J. B. Spangler, J. Tomala, V. C. Luca et al., "Antibodies to interleukin-2 elicit selective T cell subset potentiation through distinct conformational mechanisms," *Immunity*, vol. 42, no. 5, pp. 815–825, 2015.

[24] S. Létourneau, E. M. M. van Leeuwen, C. Krieg et al., "IL-2/anti-IL-2 antibody complexes show strong biological activity by avoiding interaction with IL-2 receptor alpha subunit CD25," *Proceedings of the National Academy of Sciences*, vol. 107, no. 5, pp. 2171–2176, 2010.

[25] A. L. Alaofi, "Probing the flexibility of Zika virus envelope protein DIII epitopes using molecular dynamics simulations," *Molecular Simulation*, vol. 46, no. 7, pp. 541–547, 2020.

[26] A. L. Alaofi, "Exploring structural dynamics of the MERS-CoV receptor DPP4 and mutant DPP4 receptors," *Journal of Biomolecular Structure and Dynamics*, vol. 40, no. 2, pp. 752–763, 2020.

[27] A. L. Alaofi and M. Shahid, "Mutations of SARS-CoV-2 RBD may alter its molecular structure to improve its infection efficiency," *Biomolecules*, vol. 11, no. 9, p. 1273, 2021.

[28] S. A. Ali, M. I. Hassan, A. Islam, and F. Ahmad, "A review of methods available to estimate solvent-accessible surface areas of soluble proteins in the folded and unfolded states," *Current Protein & Peptide Science*, vol. 15, no. 5, pp. 456–476, 2014.

[29] J. A. Marsh and S. A. Teichmann, "Relative solvent accessible surface area predicts protein conformational changes upon binding," *Structure*, vol. 19, no. 6, pp. 859–867, 2011.

[30] M. R. Arkin, M. Randal, W. L. DeLano et al., "Binding of small molecules to an adaptive protein-protein interface," *Proceedings of the National Academy of Sciences*, vol. 100, no. 4, pp. 1603–1608, 2003.

[31] "The PyMOL molecular graphics system," 2000, https://pymol.sourceforge.net/overview/index.htm.

[32] "Gromacs: high performance molecular simulations through multi-level parallelism from laptops to supercomputers-sciencedirect," 2022, https://www.sciencedirect.com/science/article/pii/S2352711015000059.

[33] A. L. Alaofi, "The Glu143 residue might play a significant role in T20 peptide binding to HIV-1 receptor gp41: an in silico study," *Molecules*, vol. 27, no. 12, p. 3936, 2022.

[34] T. Darden, D. York, and L. Pedersen, "Particle mesh Ewald: an N log(N) method for Ewald sums in large systems," *The Journal of Chemical Physics*, vol. 98, no. 12, pp. 10089–10092, 1993.

[35] D. Nayar, M. Agarwal, and C. Chakravarty, "Comparison of tetrahedral order, liquid state anomalies, and hydration behavior of mTIP3P and TIP4P water models," *Journal of Chemical Theory and Computation*, vol. 7, no. 10, pp. 3354–3367, 2011.

[36] J. Chen, S. Zhang, W. Wang, L. Pang, Q. Zhang, and X. Liu, "Mutation-induced impacts on the switch transformations of the GDP- and GTP-bound K-ras: insights from multiple replica Gaussian accelerated molecular dynamics and free energy analysis," *Journal of Chemical Information and Modeling*, vol. 61, no. 4, pp. 1954–1969, 2021.

[37] J. Chen, L. Wang, W. Wang, H. Sun, L. Pang, and H. Bao, "Conformational transformation of switch domains in GDP/K-Ras induced by G13 mutants: an investigation through Gaussian accelerated molecular dynamics simulations and principal component analysis," *Computers in Biology and Medicine*, vol. 135, Article ID 104639, 2021.